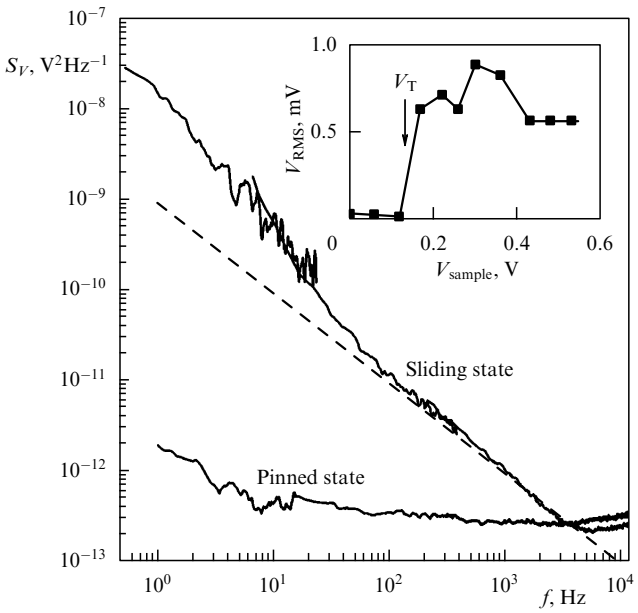

Figure 5. Noise-power spectral density of the output signal measured across an $Rb_{0.30}MoO_3$ wire at $V = 0$ V (pinned state) and at $V = 0.3$ V (sliding state). Inset: the rms noise voltage measured at different voltages.

increase in the noise voltage is observed as expected from CDW dynamics.

5. Conclusions

We have presented four-probe measurements on CDW wire structures with micron-size dimensions. Wires are made in thin films consisting of single-phase $Rb_{0.30}MoO_3$ with a granular structure. The quasi-particle resistance measured as a function of temperature clearly reveals the expected opening of an excitation gap at a Peierls temperature of 180 K. The value of the zero-temperature gap is suppressed for films with the smallest grain sizes. We clearly observe nonlinear current-voltage characteristics, indicative of the sliding of CDWs. The threshold field is much higher than reported on bulk crystals.

Finite-size effects may play a role, but the possibility of CDW depinning from grain boundaries or contact interfaces must also be considered.

Acknowledgments. We wish to acknowledge Hans Mooij, Mark Visscher, Behzad Rejaei, and Gerrit Bauer for discussions, Leo Lander for technical assistance, Jip Steinfort for X-ray analysis, and Chresten Træholt and Henny Zandbergen for TEM work. Research was supported by the Netherlands Foundation for Fundamental Research on Matter (FOM).

References

1. Grüner G *Density Waves in Solids* (Frontiers in physics Vol. 89) (Reading, Mass: Addison – Wesley Pub. Co. 1994)
2. Peierls R E *Quantum Theory of Solids* (Oxford: Clarendon Press, 1955)
3. Monceau P, in *Electronic Properties of Quasi-One-Dimensional Metals* (Ed. by P Monceau) (Dordrecht: Reidel, 1985) Vol. 2.
4. Schlenker C et al., in *Low-Dimensional Properties of Molybdenum Bronzes and Oxides* (Ed C Schlenker) (Dordrecht: Kluwer Academic Publishers, 1989) p. 159 – 257
5. Fukuyama H, Lee P A *Phys. Rev. B* **17** 535 (1978); Lee P A, Rice T M *Phys. Rev. B* **19** 3970 (1979)
6. Latyshev Yu I et al. *Phys. Rev. Lett.* **78** 919 (1997)
7. Visscher M I, Rejaei B *Phys. Rev. Lett.* **79** 4461 (1997)
8. Sinchenko A A et al. *Pis'ma Zh. Eksp. Teor. Fiz.* **64** 259 (1996) [*JETP Lett.* **64** 285 (1996)]
9. Artemenko S N, Remizov S V *Pis'ma Zh. Eksp. Teor. Fiz.* **65** 50 (1997) [*JETP Lett.* **65** 53 (1997)]
10. van der Zant H S J et al. *Appl. Phys. Lett.* **68** 3823 (1996)
11. Mantel O C et al. *Phys. Rev. B* **55** 4817 (1997)
12. Bervas E, Thèse de docteur ingenieur (Université de Grenoble, 1984)
13. Sato M et al. *J. Phys. C* **18** 2603 (1985)
14. Brütting W et al. *Phys. Rev. B* **51** 9533 (1995)
15. Borodin D V, Zaitsev-Zotov S V, Nad' F Ya *Zh. Eksp. Teor. Fiz.* **93** 1394 (1987) [*Sov. Phys. JETP* **66** 793 (1987)]
16. McCarten J et al. *Phys. Rev. Lett.* **63** 2841 (1989)
17. Xue-mei W, Dian-lin Z, Yuheng Z *Phys. Rev. B* **45** 13250 (1992)
18. Bhattacharya S et al. *Phys Rev. Lett.* **54** 2453 (1985)

Flow diagram for impurity scattering in Tomonaga – Luttinger liquids

Y Oreg, A M Finkel'stein

1. Introduction

The electron liquids in quantum wires are usually described in terms of the Tomonaga – Luttinger (TL) model [1]. Edge states in a two-dimensional electron gas, under conditions of the fractional quantum Hall effect, were argued to be TL liquids as well [2]. It is well known that in the TL model with a repulsive electron – electron (e – e) interaction the effective strength of backward scattering by an impurity defect increases with decreasing temperature [3]. For this reason, the description of a single defect in a TL liquids is based on the assumption [4 – 6] that at low temperatures the asymptotic behavior of the system may be described as tunneling between two disconnected semi-infinite TL wires. The effective amplitude of tunneling between the half-wires scales to zero with decreasing temperature, because the tunneling density of states at the ending point of a TL liquid vanishes when the e – e interaction is repulsive. This description corresponds to a scenario in which the effective strength of the impurity increases in the course of the renormalization, so that at the final stage a weak impurity transforms into a strong barrier, and disconnects the TL wire. However, a direct calculation of the tunneling density of states [7] obtained by a mapping of the weak impurity problem onto a Coulomb gas theory, apparently contradicts this intuitive picture. It has been found that at the location of a weak impurity the tunneling density of states is enhanced, rather than vanishing. The scenario in which a weak impurity eventually disconnects a TL wire assumes that no other fixed points intervene in the scaling from the repulsive fixed point of a weakly scattering defect to the attractive fixed point corresponding to a tunneling junction of two half-wires. The contradiction by this scenario of calculations of single particle properties, such as the tunneling density of states [7], and the Fermi edge singularity [8], indicates that maybe this is not the case.

In this work the problem of a single impurity in TL liquids with a repulsive e – e interaction is reinvestigated. We concentrate on the limit when the Fermi wave length is much larger than the defect size. This situation is typical for semiconductors, where the filling of the conduction band is

far from one half. Then the internal structure of the defect is not important†, and it is possible to describe the problem as a continuous model with an appropriately chosen point-like defect. We show that in the continuous model the low energy physics of a weak impurity is controlled by a fixed point that differs from a tunneling junction of two half-wires. Namely, we find here that the fixed point for infinitely strong impurity backward scattering is repulsive. This implies that there should also exist an attractive fixed point at a finite value of the backward scattering amplitude. An important fact is that the fixed point describing the tunneling junction and the two new fixed points describing backward scattering are located in different parts of the RG flow diagram. We think that the attraction of the weak impurity problem to the new fixed point is the reason for the difference between the results obtained by means of the Coulomb gas theory for the single particle correlators, and those obtained relying on the scenario of two disconnected wires.

2. Weak and strong impurities' potential limit

In this section we recall the main results concerning the renormalization of the problem in the limits of a weak and of a strong impurity potential. The Hamiltonian of the TL model in the bosonic representation is given by

$$H_{\mathrm{TL}}^{\mathrm{B}} = \frac{v_{\mathrm{F}}}{2g}\int \mathrm{d}x\left[\left(\frac{\mathrm{d}\phi}{\mathrm{d}x}\right)^2 + \left(\frac{\mathrm{d}\tilde{\phi}}{\mathrm{d}x}\right)^2\right]. \qquad (1)$$

Here the operators ϕ and its dual partner $\tilde{\phi}$ are related to the electron density and current density of the electron liquid respectively. The parameter g describes the e–e interaction; $g < 1$ when the e–e interaction is repulsive, while for the attractive interaction $g > 1$.

Let us discuss the scattering of the electrons by an impurity potential $U(x)$. For low energy physics only processes of electron scattering with a momentum transfer close to zero and to $2k_{\mathrm{F}}$ are essential. For a weak impurity the forward and backward scattering amplitudes are

$$u_+ = \int \mathrm{d}x\frac{U(x)}{v_{\mathrm{F}}}\,, \qquad u_- = \frac{|U_{2k_{\mathrm{F}}}|}{v_{\mathrm{F}}}\,,$$

where

$$|U_{2k_{\mathrm{F}}}|\exp(\mathrm{i}\varphi_u) = -\int \mathrm{d}x U(x)\exp(\mathrm{i}2k_{\mathrm{F}}x)\,.$$

For a local potential the line of the bare parameters corresponds to $u_+ \approx u_-$. In addition to u_+, u_-, and φ_u, another parameter, u_{a}, describing the asymmetry of the forward scattering of left and right movers can be introduced. In the presence of time reversal symmetry $u_{\mathrm{a}} \equiv 0$, but it is not necessarily zero for the quantum Hall edge states. The RG-equations for the backward scattering problem are

$$\frac{\mathrm{d}u_-}{\mathrm{d}\xi} = u_-(1-g)\,, \quad \frac{\mathrm{d}u_+}{\mathrm{d}\xi} = \frac{\mathrm{d}u_{\mathrm{a}}}{\mathrm{d}\xi} = \frac{\mathrm{d}\varphi_u}{\mathrm{d}\xi} = 0\,. \qquad (2)$$

These equations describe a repulsive manifold of fixed points L_0, denoted as the L_0-line at the left-bottom corner,

† On the contrary, when a tight binding model with a link defect is used to analyze the backward scattering the final fixed point depends on the internal structure of the defect (see, e.g., Ref. [9]).

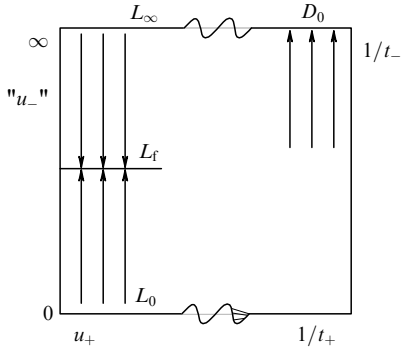

Figure 1. RG-flow diagram of a point-like defect in a quantum wire with a repulsive electron–electron interaction. The weak impurity scattering problem is represented on the left side, and the tunneling model on the right. For a local defect the two problems do not flow to each other in the model with a linearized electron spectrum. The attractive fixed line L_{f} controls the low temperature physics of the backward scattering. (For details see Section 4.)

$u_\pm \ll 1$, of the RG-plane depicted in Fig. 1. Under the condition that the impurity can be described as a local weak potential in a TL liquid, the forward scattering amplitude u_+ is a marginal parameter. In contrast to u_+, the backward scattering amplitude u_- is relevant for the repulsive case. Equation (2) were derived [4] for small u_-. The renormalization of u_- in the strong coupling regime is discussed in Sections 3 and 4.

When the bare impurity is strong enough, the description of the problem in terms of the scattering amplitudes u_-, u_+, u_a, and φ_u ceases to be adequate. On the other hand, the fact that the impurity is strong does not contradict the assumption of locality $k_{\mathrm{F}}a \ll 1$. A local and strong impurity can also be considered as a point-like problem, but now it should be described by two semi-infinite TL liquids, with a weak tunneling junction between their ending points. Like in the case of the weak potential scattering, there are four parameters that describe the tunneling and reflection processes at the tunneling junction of the two half-wires. These parameters are the tunneling amplitude t_-, its phase φ_t, and the two parameters, t_+ and t_{a}, characterizing the phases that an electron acquires when it is reflected at the ends of the half-wires. The parameter t_{a} describes the asymmetry of the left and the right parts of the tunneling junction. In the particular case of a strong δ-function potential, where $u_\pm = u \gg 1$, the amplitudes $t_\pm \sim 1/u$.

The low energy physics of each semi-infinite wire may be described by a single chiral mode [4, 10]. It will be assumed that there is no density–density interaction between the half-wires, but inside each of them the density–density interaction is present. The RG-equations for the tunneling problem are analogous to Eqn (2):

$$\frac{\mathrm{d}t_-}{\mathrm{d}\xi} = t_-\left(1-\frac{1}{g}\right), \quad \frac{\mathrm{d}t_+}{\mathrm{d}\xi} = \frac{\mathrm{d}t_{\mathrm{a}}}{\mathrm{d}\xi} = \frac{\mathrm{d}\varphi_{\mathrm{t}}}{\mathrm{d}\xi} = 0\,. \qquad (3)$$

In contrast to u_-, the tunneling amplitude t_- scales to zero for the repulsive e–e interaction ($g < 1$). Therefore, the manifold of fixed points describing the tunneling problem is attractive. In the two-dimensional plot depicted in Fig. 1 it is presented in the upper right corner as the D_0-line.

3. A mapping onto a spin-1/2 semi-infinite chain

In this section the problem of a local impurity in the TL model is mapped onto a semi-infinite spin-1/2 Heisenberg chain, with a magnetic field $h \propto u_-$ acting on a spin located at the origin of the chain. The mapping onto a spin chain is an appropriate way to study the nature of the strong coupling regime for the amplitude u_-.

It is convenient to describe a point-like impurity scattering by a pair of chiral variables [10]

$$\Theta_{\rm e}(x) = \frac{1}{2\sqrt{2}}\left[\tilde{\phi}(x) + \tilde{\phi}(-x) - \phi(x) + \phi(-x)\right],$$
$$\Theta_{\rm o}(x) = \frac{1}{2\sqrt{2}}\left[\tilde{\phi}(x) - \tilde{\phi}(-x) - \phi(x) - \phi(-x)\right]. \tag{4}$$

In terms of self dual operators $\Theta_{\rm e}$ and $\Theta_{\rm o}$ the scattering Hamiltonian can be rewritten in the form

$$H = H_{\rm e} + H_{\rm o},$$
$$H_{\rm o} = \frac{v_{\rm F}}{g}\int {\rm d}x\left[\left(\frac{\partial\Theta_{\rm o}}{\partial x}\right)^2 - \frac{u_- g}{\pi\eta}\cos(\beta\sqrt{2}\Theta_{\rm o})\delta(x)\right],$$
$$H_{\rm e} = \frac{v_{\rm F}}{g}\int {\rm d}x\left[\left(\frac{\partial\Theta_{\rm e}}{\partial x}\right)^2 - \frac{u_+\beta g}{\sqrt{2}\pi}\,\frac{\partial\Theta_{\rm e}(x)}{\partial x}\delta(x)\right]. \tag{5}$$

Although $\Theta_{\rm e}$ and $\Theta_{\rm o}$ do not commute, $\left[\Theta_{\rm e}(x), \Theta_{\rm o}(y)\right] = -{\rm i}/4$, the Hamiltonian H is divided into even and odd parts, because the even part, $H_{\rm e}$, contains only derivatives. For simplicity we omit the phase φ_u, and the $u_{\rm a}$-term related to time reversal asymmetry, in $H_{\rm o}$.

We now show that the odd part $H_{\rm o}$ is effectively equivalent to the Hamiltonian of a semi-infinite spin-1/2 antiferromagnetic chain with anisotropy $\overline{\gamma}$:

$$H_S = \frac{J}{2}\sum_{n=0}^{\infty}\left(S_n^+ S_{n+1}^- + S_n^- S_{n+1}^+\right) + \overline{\gamma}J\sum_{n=0}^{\infty}\left[\left(S_n^+ S_n^- - \frac{1}{2}\right)\right.$$
$$\left.\times\left(S_{n+1}^+ S_{n+1}^- - \frac{1}{2}\right)\right] - hJ\left(S_0^- + S_0^+\right). \tag{6}$$

A Hamiltonian of this type, with $\overline{\gamma} = 0$, was introduced by Guinea [11] for the description of a quantum particle interacting with a dissipative environment, at a particular value of the friction coefficient. It has also been used to discuss the transmission through barriers in TL liquids [4], for a given value of the e–e interaction $g = 1/2$. Here we introduce the $\overline{\gamma}$-term in order not to be limited to a particular value of the e–e interaction.

To show the equivalence of $H_{\rm o}$ and H_S, one should perform a sequence of transformations. After applying the inverse of the Jordan–Wigner transformation [12], H_S transforms in a standard way into

$$H_c = \frac{J}{2}\sum_{j=0}^{\infty} c_j^\dagger c_{j+1} + {\rm H.c.} + \overline{\gamma}J\sum_{j=0}^{\infty}\left[\left(n_j - \frac{1}{2}\right)\right.$$
$$\left.\times\left(n_{j+1} - \frac{1}{2}\right)\right] - hJ\left(c_0^\dagger + c_0\right), \tag{7}$$

where the fermion system H_c is at half filling. The continuum limit of H_c (e.g., see Ref. [12]) corresponds to the effective Hamiltonian $H_c^{\rm cont} = H_0 + H_{\rm int} + H_{\rm Um} + H_h$, where

$$H_0 = {\rm i}v_{\rm F}\int_0^\infty {\rm d}x\left(L^\dagger\partial_x L - R^\dagger\partial_x R\right),$$

$$H_{\rm int} = v_{\rm F}\overline{\gamma}\int_0^\infty {\rm d}x\left(\overline{\rho}_{\rm L}^2 + \overline{\rho}_{\rm R}^2 + 4\overline{\rho}_{\rm R}\overline{\rho}_{\rm L}\right),$$

$$H_{\rm Um} = -2\overline{\gamma}v_{\rm F}\int_0^\infty {\rm d}x\left[(R^\dagger L)^2 + (L^\dagger R)^2\right],$$

$$H_h = v_{\rm F}\frac{1}{\sqrt{\eta}}\,h\left[R(0) + L(0) + R^\dagger(0) + L^\dagger(0)\right].$$

Here $v_{\rm F} = J\eta$, where η is the lattice spacing, and the operators L and R represent left and right movers on a semi-infinite line. The remnant of the discrete structure of the chain is the term $H_{\rm Um}$ which corresponds to the Umklapp processes at half filling. This Umklapp term scales to zero for $|\overline{\gamma}| < 1$. It also renormalizes the parameters of $H_{\rm int}$. But at small $\overline{\gamma}$ the latter effect is negligible, and therefore one may ignore $H_{\rm Um}$. The last step which needs to be carried out is to unfold the semi-infinite line with left and right movers into a full line with a single chiral bosonic field. After diagonalizing the quadratic part of the Hamiltonian, we find:

$$\overline{H}_{\rm chiral} = \frac{v_{\rm F}}{g_{\rm ch}}\int_{-\infty}^{\infty} {\rm d}x\left[\pi\overline{\rho}_{\rm ch}^2(x)\right.$$
$$\left. - \frac{4g_{\rm ch}}{\sqrt{2\pi}\eta}\,h\cos\left[\beta_{\rm ch}\overline{\Theta}_{\rm ch}(x)\right]\delta(x)\right], \tag{8}$$

where ${\rm d}\overline{\Theta}_{\rm ch}(x)/{\rm d}x = \sqrt{\pi}\,\overline{\rho}_{\rm ch}(x)$, $\beta_{\rm ch} = \sqrt{4\pi}\exp\chi$,

$$\chi = \frac{1}{2}{\rm arctanh}\left(\frac{2\gamma}{\pi + \overline{\gamma}}\right), \quad g_{\rm ch} \approx \left(1 + \frac{\overline{\gamma}}{\pi}\right)^{-1}.$$

Notice, the important role of the $\overline{\gamma}$-term — it modifies $\beta_{\rm ch}$ inside the cosine term.

Thus, as a result of the sequence of transformations

$$H_S \to H_c \to H_c^{\rm cont} \to \overline{H}_{\rm chiral} \to H_{\rm o} \tag{9}$$

we obtain that the Hamiltonians H_S and $H_{\rm o}$ are equivalent when $\beta_{\rm ch} = \sqrt{2}\beta$ and $h = u_-(8\pi)^{-1/2}$. Due to the $\overline{\gamma}$-term, this equivalence is extended here to a finite interval of the e–e interaction.

We will use the equivalence of $H_{\rm o}$ and H_S to analyze the stability of the fixed line at $u_- = \infty$ and small u_+. A variant of the Noziéres and Blandin approach [13] in their analysis of the two channel Kondo problem will be considered. Following this approach, we will assume that $h \gg 1$, and check whether the fixed point $h = \infty$ is a stable one. In the presence of a strong magnetic field $h \gg 1$, the spin at site 0 is oriented along the direction opposite to the magnetic field. Its coupling to the nearest neighbor at the lattice site 1, can be treated as a perturbation. After performing the permutation $x \to z$, $y \to x$, and $z \to y$ the reduced Hamiltonian that includes only sites 0 and 1 is given by

$$H_S^{01} = JS_0^z S_1^z + \frac{J}{4}(1 - \overline{\gamma})\left[S_0^+ S_1^+ + S_0^- S_1^-\right]$$
$$+ \frac{J}{4}(1 + \overline{\gamma})\left[S_0^- S_1^+ + S_0^+ S_1^-\right] - 2hJS_0^z. \tag{10}$$

For $h \gg 1$ the spin at site 0 is in the state $|0\uparrow\rangle$. Up to the first order in J we have $\langle 1\downarrow|\langle 0\uparrow|H_S^0|0\uparrow\rangle|1\downarrow\rangle = -J/4$ and $\langle 1\uparrow|\langle 0\uparrow|H_S^0|0\uparrow\rangle|1\uparrow\rangle = J/4$. This means that the spin at site 1 is under the action of an effective magnetic field $\tilde{h} = -1/4$. Under the assumption that $h \gg 1$, the higher orders in the perturbation theory give small corrections to $\tilde{h}$, of the order of

h^{-1}. As a result of this renormalization procedure step, we arrive at a problem equivalent to the initial one: a semi-infinite spin-1/2 Heisenberg chain, with a local magnetic field acting on the site at the origin of the chain (now it will be site 1).

If one assumes that the discussed fixed point is such that the local magnetic field at the origin of the spin chain flows to infinity, then the renormalization procedure generates a relevant operator that makes this process non-convergent. This is in contradiction with the initial assumption that $h = \infty$ is a stable fixed point. We have to conclude that $h = \infty$ is a repulsive fixed point. This conclusion holds for a finite interval of the parameter $|\bar{\gamma}| \lesssim 1$, because $\bar{\gamma}$ does not radically influence the effective magnetic field acting on site 1.

It is not accidental that the present discussion resembles the analysis of the overscreened two channel Kondo problem [13]. Indeed, the spin chain model, in the absence of the $\bar{\gamma}$-term, is equivalent to the TL-impurity problem at a particular value of the e–e interaction parameter $g = 1/2$, [4, 11]. The latter problem can in turn be reduced to a resonant level model [14]. The overscreened two channel Kondo model at a specific value of the longitudinal exchange coupling is equivalent to the resonant level model as well [15]. Thus, the spin chain model and the Kondo model are equivalent at one point. On the other hand, it is well known that in the overscreened two channel Kondo problem the limit of infinite exchange interaction is unstable, and there is an anomalous fixed point at a finite coupling [13]. This property is preserved in the presence of a spin exchange anisotropy, which is irrelevant [16]. Since the spin chain model and the two channel Kondo model are equivalent at one point, it is natural that we have found that the point $h = \infty$ is repulsive. Since $h \propto u_-$, it follows from this analysis that the line L_∞ corresponding to $u_- \gg 1$ is a repulsive fixed line for the problem of impurity scattering in a TL liquid. The present treatment is not restricted to the special point of a TL liquid with $g = 1/2$. This has been accomplished by the $\bar{\gamma} \neq 0$ term in the spin chain model.

4. The unified RG flow diagram

The information collected up to now is presented in the combined plot as Fig. 1. In this plot, the scattering model is presented on the left side, and the tunneling model on the right. Since for a large barrier the backscattering amplitude is large, and the tunneling amplitude is small, we use the vertical axis to represent u_- and $1/t_-$. The horizontal axis represents u_+ together with the other parameters, which in a model with a linearized electron spectrum are not renormalized. To complete the central part of the flow diagram, a region of an intermediate impurity strength should be studied. None of the two limiting models describes the problem faithfully in this crossover region, and a consideration of a more comprehensive Hamiltonian, which covers both limiting cases, is needed. Moreover, to study the RG-flow in the crossover region, one has to give up the approximations of the linearized electron spectrum and/or of the locality of the defect. (In the bosonized representation the curvature of the electron spectrum is described by terms $\propto \rho_{\mathrm{L}}(\mathrm{R})^3$. To consider the nonlocality of the impurity one may add a term

$$\propto \psi_{\mathrm{R}}^{\dagger}(0)\,\frac{\mathrm{d}}{\mathrm{d}x}\,\psi_{\mathrm{L}}(0) + \mathrm{H.c.}\,;$$

when $k_{\mathrm{F}}a \ll 1$ the coefficient of this term is very small.) Effects arising due to the nonlinearity of the electron spectrum and the nonlocality of the defect should be studied by a loop expansion in higher orders. These effects may have highly important influence on the renormalization of the parameters u_+ and u_-, because the decoupling of forward and backward scattering is no longer valid. As a result it may cause the flow lines near the L_{f}-line to bend to the left or right.

The plot in Fig. 1 is based on the idealized models, and as a draft it gives a hint how the known limiting cases could be matched together. Since the curvature of the electron spectrum is not universal, different scenarios can occur. The two most apparent versions of the flow diagram are presented in Figs 2a and 2b, but more sophisticated variants can be imagined due to the multidimensionality of the problem, which up to now was hidden by the linearized spectrum approximation together with the locality of the defect. In the version presented in Fig. 2a, the limiting cases of a weak and a strong impurity are not connected by flow trajectories. In contrast, the RG-flow presented in Fig. 2b corresponds to a scaling from L_0 to D_0, i.e., from a weak impurity scattering to the limit of two disconnected half-wires, as was assumed in Ref. [4]. However, this version of the RG-flow acquires, in the present discussion, a new essential element. Namely, the flow trajectory after the first stage where it reaches the L_{f} -line dwells at length in its vicinity, and this leads to an intermediate asymptotic behavior. For a weak enough impurity this intermediate regime can be very long, and then it determines the low energy physics in a certain temperature range.

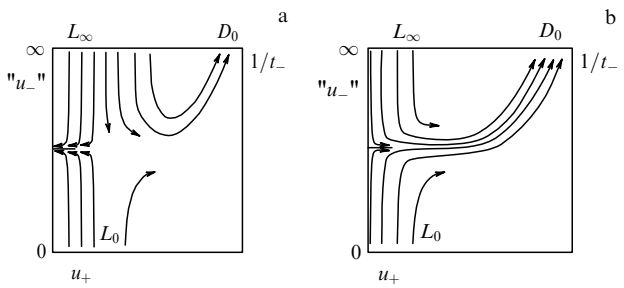

Figure 2. Two possible modifications of the flow diagram that can occur beyond the approximations of the model, such as the linearization of the spectrum, the locality of the defect, etc. The flow diagram becomes dependent on the model parameters in a non-universal way.

We emphasize that in considerations of a local defect within a linearized electron spectrum approximation, RG-trajectories that start at L_0 end at L_{f}. This approximation has been utilized in the mapping of the problem onto a Coulomb gas theory [7, 8]. Therefore, the tunneling density of states, and the Fermi edge singularity exponent, found in Refs [7, 8] correspond to the physics near L_{f}, and not to a tunneling junction, i.e., not near D_0.

5. Conclusions

We have studied a single impurity in TL liquids with a repulsive e–e interaction. The problem has been described by a continuous model with a point-like defect. Apart from the backward scattering amplitude for a weak impurity, and the tunneling amplitude at the opposite extreme, another

parameter characterizing the 'strength' of the impurity potential controls the RG-flow. The unified plot of the flow diagram is rather rich. The flow diagram contains a new attractive fixed line, L_f, controlling the low temperature physics when the bare potential of the impurity is weak. The existence of the attractive line L_f at an intermediate value of the parameter u_-, follows from the fact that both limiting lines L_∞ and L_0, have proved to be unstable. The presentation of the phase diagram in the space of parameters characterizing the impurity potential, helps clarify the difference between the D_0- and the L_f- lines of fixed points — they are located in different parts of the phase diagram.

The scenario of Ref. [4] is based on the assumption of scaling from a weak impurity scattering to a strong barrier. The existence of the novel line of fixed points, the L_f-line, indicates that the situation is more complicated (see Figs 2a, 2b). We believe that the physics of the L_f-line (that is different from the physics of two weakly connected semi-infinite lines described by D_0) may be related to the strengthening of the role of the Friedel oscillations in the TL model [5]. We think that the attraction to L_f, but not to D_0, is the reason for the results obtained by means of the Coulomb gas theory for the tunneling density of states and the Fermi edge singularity [7, 8].

To conclude, we identify a new attractive fixed point controlling the strong coupling regime of the backward scattering by a single local defect in the TL model. This novel point may also have implications for some other related problems, in particular to the theory of the motion of a quantum particle in a dissipative environment. For a more detailed version of the paper see Ref. [17].

Acknowledgments. We thank D E Khmel'nitskiĭ and Y Gefen for useful discussions. A F is supported by the Barecha Fund Award. This work is supported by the Israeli Academy of Sciences under the Grant No. 801/94-1 and by German–Israeli Foundation (GIF).

References

1. Mattis D C (Ed.) *The Many — Body Problem: an Encyclopedia of Exactly Solved Models in one Dimension* (Singapore: World Scientific, 1993) Ch. 4
2. Wen X-G *Phys. Rev. B* **44** 5708 (1991)
3. Mattis D C *Phys. Rev. Lett.* **32** 714 (1974)
4. Kane C L, Fisher M P A *Phys. Rev. Lett.* **68** 1220 (1992); *Phys. Rev. B* **46** 15233 (1992)
5. Matveev K A, Yue D, Glazman L I *Phys. Rev. Lett.* **71** 3351 (1993)
6. Furusaki A, Nagaosa N *Phys. Rev. B* **47** 4631 (1993)
7. Oreg Y, Finkel'stein A M *Phys. Rev. Lett.* **76** 4230 (1996)
8. Oreg Y, Finkel'stein A M *Phys. Rev. B* **53** 10928 (1996)
9. Eggert S, Affleck I *Phys. Rev. B* **46** 10866 (1992)
10. Affleck I, Ludwig A W *J. Phys. A: Math. Gen.* **27** 5375 (1994)
11. Guinea F *Phys. Rev. B* **32** 7518 (1985)
12. Fradkin E, in *Field Theories of Condensed Matter Systems* (Frontiers in Physics Vol. 82) (Redwood City, Calif: Addison-Wesley Pub. Co., 1991) Ch. 4
13. Nozieres Ph, Blandin A *J. Phys.* (Paris) **41** 193 (1980)
14. Matveev K A *Phys. Rev. B* **51** 1743 (1995)
15. Emery V J, Kivelson S *Phys. Rev. B* **46** 10812 (1992)
16. Affleck I et al. *Phys. Rev. B* **45** 7918 (1992)
17. To be published in *Philosophical Magazine, in the Proceedings of the "Minerva Workshop on Mesoscopics, Fractals and Neural Networks", Eilat, Israel, March 1997* (cond-mat/9707162)

Ground states in one-dimensional electron systems

W Hansen, D Schmerek, C Steinebach

The screening properties of a low-dimensional electron system in heterostructures can be rather directly probed by measurement of the capacitance between a metallic front electrode and the electron system. In this way very valuable information on the density of states (DOS) of the electron system are acquired as demonstrated in a number of publications on the DOS in electron systems of two [1, 2] or even fewer [3–7] dimensions. For an unambiguous and even quantitative analysis of the data it is crucial that the time in which charge equilibrium in the system is established is much shorter than the period over which the capacitance signal is measured. This is generally not the case if the charge exchange takes place by transport within the low-dimensional system. At high magnetic fields the capacitance signal then incorporates transport properties in the electron system with peculiar behavior at even filling factors where the diagonal conductivity vanishes [8–11]. On the other hand special heterojunction devices are developed that contain a back contact from which charge injection into the low-dimensional electron system takes place at high rates even in high magnetic fields. In this contribution we would like to summarize a number of experiments performed on such devices with electron channels of different widths. The results demonstrate that the gate voltage dependence of the capacitance reflects the formation of edge states [12, 13] and — at even smaller channel width — spatial quantization into one-dimensional (1D) subbands.

In Figure 1 a cross section and a top view of the metal insulator semiconductor (MIS) devices used for our experiments is sketched. The heterojunction samples are grown by molecular beam expitaxy and contain an Si-doped back contact, a GaAs spacer, a barrier formed by an AlAs/GaAs superlattice a thin GaAs cap layer and thermally evaporated gate electrodes that are finely patterned by electron beam lithography [6]. The layer thicknesses of the GaAs spacer layer, the barrier and the cap are 100 nm, 37 nm and 5 nm, respectively. The gate electrodes form a 150 μm long center

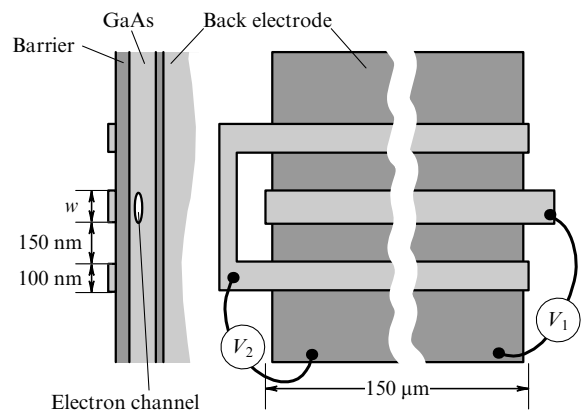

Figure 1. Cross section and top view of a MIS heterojunction device for the investigation of narrow electron channels. In the top view light areas represent the front electrodes and the dark area — the back contact. The thicknesses of the barrier and the separation between the gate and back electrode are, respectively: $d = 42$ nm and $D = 142$ nm.